Ohmori, T., et al., *Transmutation in the electrolysis of lightwater - excess energy and iron production in a gold electrode*. Fusion Technol., 1997. **31**: p. 210.

TRANSMUTATION IN THE ELECTROLYSIS OF LIGHT WATER – EXCESS ENERGY AND IRON PRODUCTION IN A GOLD ELECTRODE

NUCLEAR REACTIONS IN SOLIDS

TADAYOSHI OHMORI *Hokkaido University*
Catalysis Research Center, Kitaku Sapporo 060, Japan

MICHIO ENYO *Hakodate National College of Technology*
Tokuracho Hakodate 042, Japan

TADAHIKO MIZUNO *Hokkaido University*
Faculty of Engineering, Kitaku Sapporo 060, Japan

YOSHINOBU NODASAKA *Hokkaido University*
School of Dentistry, Kitaku Sapporo 060, Japan

HIDEKI MINAGAWA *Hokkaido National Industrial Research Institute*
Toyohiraku Sapporo 062, Japan

Received January 29, 1996
Accepted for Publication June 14, 1996

KEYWORDS: iron production, excess energy, isotopic abundance

The identification of some reaction products possibly produced during the generation of excess energy is attempted. Electrolysis is performed for 7 days with a constant current intensity of 1 A. The electrolytes used are Na_2SO_4, K_2SO_4, K_2CO_3, and KOH. After the electrolysis, the elements in the electrode near the surface are analyzed by Auger electron spectroscopy and electron probe microanalysis. In every case, a notable amount of iron atoms in the range of 1.0×10^{16} to 1.8×10^{17} atom/cm^2 (true area) are detected together with the generation of a certain amount of excess energy evolution. The isotopic abundance of iron atoms, which are 6.5, 77.5, and 14.5% for ^{54}Fe, ^{56}Fe, and ^{57}Fe, respectively, and are obviously different from the natural isotopic abundance, are measured at the top surface of a gold electrode by secondary ion mass spectrometry. The content of ^{57}Fe tends to increase up to 25% in the more inner layers of the electrode.

INTRODUCTION

The nuclear transmutation that occurs in a metal cathode during electrolysis seems to be essentially different from conventional nuclear transmutation. Its most striking characteristic is that the radiation emission from the reaction zone is either lacking or extremely small. Perhaps the energies generated in this reaction zone are dispersed to surrounding atoms; this dispersion possibly acts as a driving force for further transmutations. Therefore, it is thought that the possibility of some nuclear transmutation other than a hydrogen-deuterium, deuterium-deuterium, or tritium-deuterium fusion reaction should be taken into account in such a system. Actually, based on analysis using secondary ion mass spectrometry (SIMS) and inductively coupled plasma-mass spectroscopy (ICPMS), Bush and Eagleton[1] and Bush[2] have reported that calcium and strontium atoms are produced from K^+ and Rb^+ ions, respectively, in the electrolysis of light water with a nickel cathode. The result, however, is not generally accepted because of the difficulty of excluding the possibility of hydride formation of these metals. On the other hand, we recently observed the production of iron atoms reaching 1.0×10^{16} to 1.8×10^{17} atom/cm^2 (true area) together with the excess energy evolution of 215 to 723 mW for gold cathodes after the electrolysis of light water.[3,4] To verify that the production of iron atoms is induced because of some nuclear transmutation, one absolutely must investigate the isotopic abundance of the aforementioned iron atoms.

For this reason, we made a quantitative analysis and an isotopic quantification of all the elements including iron (mass number <200) in a gold cathode after the electrolysis of light water. In this work, we also measured the excess energies and checked the correlation with the amounts of reaction products.

EXPERIMENT

Five fused quartz [iron < 0.3 parts per million (ppm)] electrolytic cells were used. These were in the form of a flat-bottomed cylinder (~19.6 cm^2 × 15 cm) with a 5-cm-thick silicone rubber stopper holding a working electrode, a counter electrode, a thermocouple, and a quartz glass inlet tube for H_2 gas, which were cleaned carefully with hot mixed acid (1:1 H_2SO_4, HNO_3), rinsed with MQ water ultrasonically, and finally rinsed with MQ water before conducting the electrolysis. The working electrode was suspended by a gold lead wire (0.03-cm diameter) coated with thin Teflon film without its terminal parts.

The five cells were placed in either of two types of air thermostats, whose temperature was regulated at ~21°C. The temperature fluctuation of one thermostat was periodical, that is, ±0.5°C with 10 cycle/h, so that the fluctuation of the solution temperature in the electrolytic cell placed in this thermostat was kept within ±0.03°C. While the temperature in another thermostat fluctuated by ±0.5°C with 1 cycle/day, the fluctuation of the solution temperature in this thermostat needed to be depressed within ± 0.03°C if the correction of the foregoing periodical temperature fluctuation was to be made.

The working electrodes used were cold-worked gold sheets (which had an apparent area of 2.5 and 5.0 cm^2, were 0.1-mm thick, and had 99.99% purity and iron <1 ppm), whose surface was scraped with a cleaned glass fragment edge and then washed with methyl alcohol and MQ water. The roughness factor of the electrode determined from the measurement of double-layer capacitance[5] was 2.0. The counter electrode was a 1- × 7-cm, 80-mesh platinum net (with 99.98% purity and iron <16 ppm). The working and the counter electrodes were placed at the bottom of the cell to minimize the temperature gradient in the electrolyte solution by vigorously stirring with H_2 and O_2 bubbles evolved from these electrodes. The electrolyte solutions used were 0.5 *M* Na_2SO_4, K_2SO_4, K_2CO_3, and KOH, which were prepared from Merck Sprapur-grade chemicals. The volume of the electrolyte solution was 100 ml. The electric heater for measuring the calibration curves between the increment of the solution temperature and the input power was a Ni-chrome spiral (0.3- and 1.6-mm diameter) connected to copper wires (1-mm diameter), both ends of which were inserted into a Pyrex glass sheath (of 6-mm diameter and 15-cm length) containing silicone oil. When the calibration curves were measured, the heater was set at the position of the working electrode. During the measurement of the calibration curves, the solution was stirred by passing H_2 gas with the same flow rate as that of the H_2 and O_2 gases evolved in the real electrolysis. The electrolysis was conducted galvanostatically for 7 days at a constant current of 1 A, and the applied cell voltage and the increase in solution temperature were monitored by a recorder. Before the electrolysis, the gold electrode was kept at RHE by passing H_2 gas into the cell. During the electrolysis, MQ water was added every 24 h to maintain the total amount of the solution.

To identify the elements present in the gold electrodes after electrolysis and to determine these isotopic abundances, we carried out Auger electron spectroscopy (AES), electron probe microanalysis (EPMA), and SIMS measurements. The AES measurement was made with the use of an ANELVA AAS-200 Auger electron spectrometer with 3.0-keV beam energy and 2.5-A filament current. The electrode sample after having been washed with MQ water was placed on a nickel plate holder in a chamber equipped with electron and ion guns in a vacuum of 2×10^{-8} Torr. The Ar^+ ion bombardment was performed under 2.5×10^{-5} Torr of 99.9995% argon gas. The pictures of the mapping of the reaction product (iron) in the electrode were obtained by means of scanning electron microscopy (SEM) (Hitachi S-4000) and EPMA (SHIMADZU EMX-SM and 25-kV accelerating voltage). The SIMS measurement was carried out with a HITACHI IMA-3 ion microanalyzer under 5×10^{-9} Torr by O_2^+ ion irradiation (100-nA primary ion current and 12-keV accelerating voltage) from Hitachi Instruments Engineering Company.

RESULTS AND DISCUSSION

Heat Measurement

A typical calibration curve of the electrolytic cell between the increment of the solution temperature and the input power is shown in Fig. 1. A very reproducible linear relationship was

obtained up to ~17°C in each cell. The cell constants of the five cells calculated from the gradient of such linear relationships were 3.08, 3.10, 3.40, 3.53, and 3.47, the precision of which was ±0.04. The change of the cell constants with losing solution volume within 10 ml (the amount of which corresponds approximately to that lost through the electrolysis for 1 day) was practically negligible.

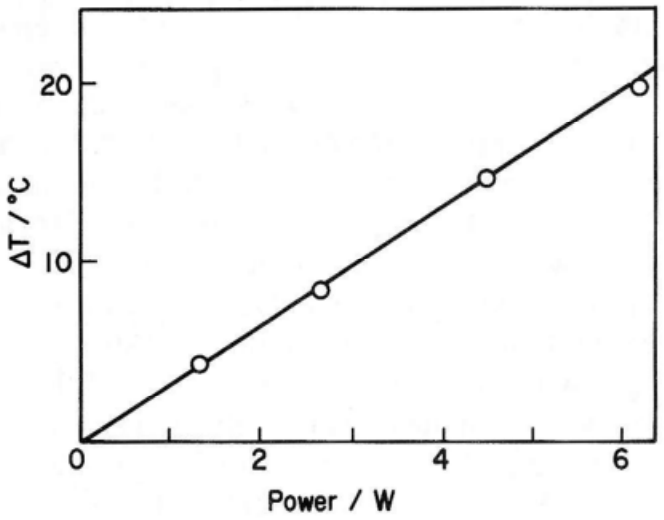

Fig. 1. The calibration curve between the input power and the solution temperature rise.

When the increment of the solution temperature ΔT was lower than 17°C, the rate of excess energy evolution R_{ex} was determined by the following equation[4]:

$$R_{ex} = \Delta T/k - (R_{app} - E_{th}I), \quad (1)$$

where

R_{app} = applied electrolysis power

I = electrolysis current

E_{th} = thermoneutral potential, that is, 1.48 V for H_2O decomposition.

On the other hand, when ΔT exceeded 17°C, the R_{ex} was determined from the difference between the input power of the calibration curve and $(E + E_{th})I$, which is necessary to keep the solutions in the calibration and the electrolytic cells at a given temperature.

Figure 2 shows the typical time courses of the solution temperature rise after starting electrolysis in the Na_2SO_4 and K_2CO_3 solutions. Figure 2 also shows the time elapse of the cell voltage. As one can see, the increase in the solution temperature in Na_2SO_4 is clearly larger than that in K_2CO_3, although the cell voltages are nearly the same in both cases. This difference was essentially unchanged over the entire time of the electrolysis. This result directly shows that

excess energy is steadily evolved at least during the electrolysis with the gold electrodes in the Na_2SO_4 solutions.

The R_{ex} obtained in the various electrolyte solutions are listed in Table I. The maximum R_{ex} obtained was 937 mW (2.5 cm^2 gold in Na_2SO_4), which corresponds to 22% of the applied input power. The values of R_{ex} on eleven 5-cm^2 gold/electrolyte systems and on nine 2.5-cm^2 gold/electrolyte systems are in the ranges of 185 to 710 and 255 to 937 mW, respectively, the amount of which seems to be somewhat increasing with increasing electrolysis current density. These values fairly reproduce the results obtained for the gold electrode in the K_2CO_3, Na_2CO_3, and Li_2SO_4 solutions.[3,4] Measurement of the current efficiency was made repeatedly at a given time during the electrolysis, the result of which was 100.6, 100.1, and 101.1%. This fact shows that there is no conceivable possibility of the recombination of H_2 and O_2 as another cause of the excess energy production.

TABLE I
Results of the Heat Measurement

Electrode	Solution	R_{app} - 1.48I (W)	R_{ex} (mW)	$\frac{R_{ex}}{R_{app}R - 1.48I}$ (%)
Gold (10 cm^2)	Na_2SO_4	3.70	710	19
		3.68	353	10
		3.79	534	14
		4.00	580	15
		3.72	625	17
		3.72	343	9
		3.40	215	6
		3.44	218	6
	K_2CO_3	4.36	428	10
	KOH	4.28	185	4
Gold (5 cm^2)	Na_2SO_4	4.19	937	22
		4.03	615	15
		4.38	600	14
		4.28	795	19
	K_2CO_3	4.48	744	17
		4.12	528	13
		3.83	713	19
	K_2SO_4	4.43	401	9
		4.12	255	6

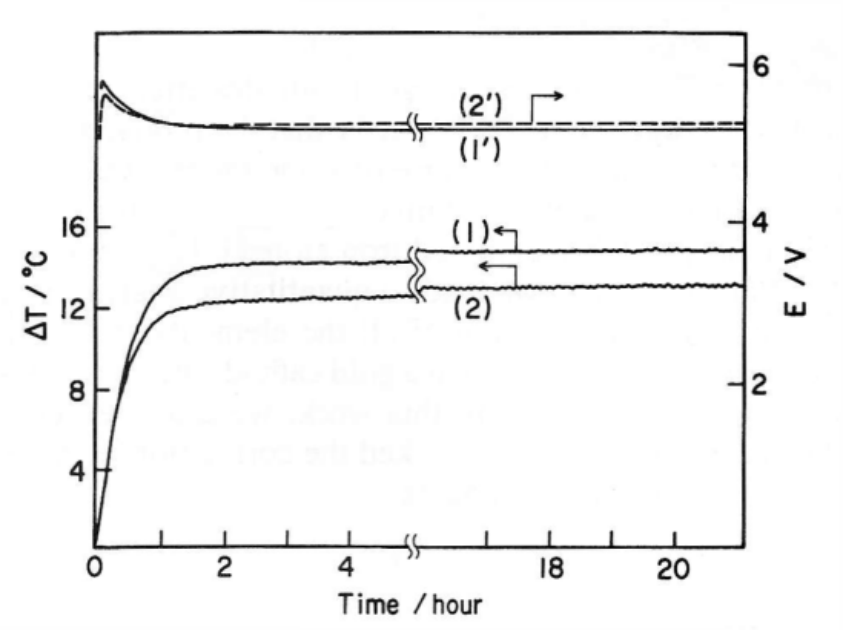

Fig. 2. The time elapse of the solution temperature and the input potential after the electrolysis: Na_2SO_4 (1) and (1′), and K_2CO_3 (2) and (2′).

The results of the R_{ex} measurement on gold and platinum electrodes in the 0.5 M H_2SO_4 solutions are listed in Table II. The values of R_{ex} were negative, but the efficiency compared with the applied power was close to 0 in every case. This shows that practically no excess heat was evolved in the H_2SO_4 solutions. So far, hardly any papers have reported the evolution of excess energy in acid solutions, which means that there is no excess energy evolution. Practically without exception, we observed in the H_2SO_4 solutions no excess energy evolution. The reliability of our heat measurements is supported.

TABLE II
Results of the Heat Measurement

Electrode	Solution	$R_{app} - 1.48\ I$ (W)	R_{ex} (mW)	$\frac{R_{ex}}{R_{app}R - 1.48I}$ (%)
Gold	H_2SO_4	1.62	-9	-0.6
		1.62	-12	-0.7
		1.35	-9	-0.7
Platinum		1.47	-30	-2.0

The total excess energies evolved during 7 days of electrolysis are estimated to be in the range of 111 to 567 kJ from the data shown in Table I. This means that at least several moles of reaction products should be produced during the electrolysis if the excess energies are caused by some exothermic conventional chemical reaction. However, such a large amount of reaction

products was not obtained except for H_2 and O_2, which suggests that some anomalous reaction was connected with the excess energy evolution.

Reaction Product

Figures 3 and 4 show the AES spectra of the gold electrodes after 7 days of electrolysis in the Na_2SO_4 and K_2CO_3 solutions, respectively. On the spectra of the top surface (no Ar^+ ion bombardment treatment), rather than gold signals, iron and oxygen signals were observed. On carrying out Ar^+ ion bombardment, the iron and oxygen signals declined and disappeared after several minutes of the bombardment. The iron and oxygen signals were observed for every electrode independent of the nature of the electrolyte solutions. In some cases, carbon and platinum signals were observed. However, signals of other elements were not detected.

The oxygen signal always appeared together with the iron signals, and the ratio of these signal intensities was nearly the same in every AES spectrum obtained. The spectrum of pure iron (99.99%) after 30 min of Ar+ ion bombardment is shown in Fig. 5. In this spectrum, the oxygen signal appears together with the iron signals, and the shape of the oxygen and iron signals is like those shown in Figs. 3 and 4. From this fact, one can see that oxygen atoms are positioned not on gold atoms but on iron atoms. Perhaps traces of O_2 contained in argon gas were bound to iron atoms during the Ar^+ ion bombardment. When estimating the total number of iron atoms, we considered that the number of oxygen atoms estimated from the oxygen signal was equal to the number of iron atoms covered with oxygen atoms and added the number of oxygen atoms to the number of iron atoms estimated from the iron signal itself, assuming that oxygen atoms are bound to iron atoms at a ratio of 1:1.

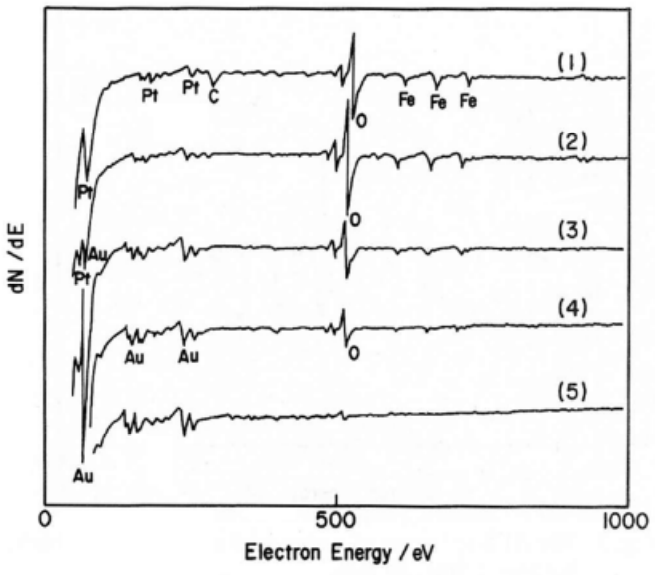

Fig. 3. The AES spectra in the electrode near the surface after the electrolysis in the Na_2SO_4 solution: Ar^+ ion bombardment time, nothing (1), 30 s (2), 120 s (3), 180 s (4), and 600 s (5).

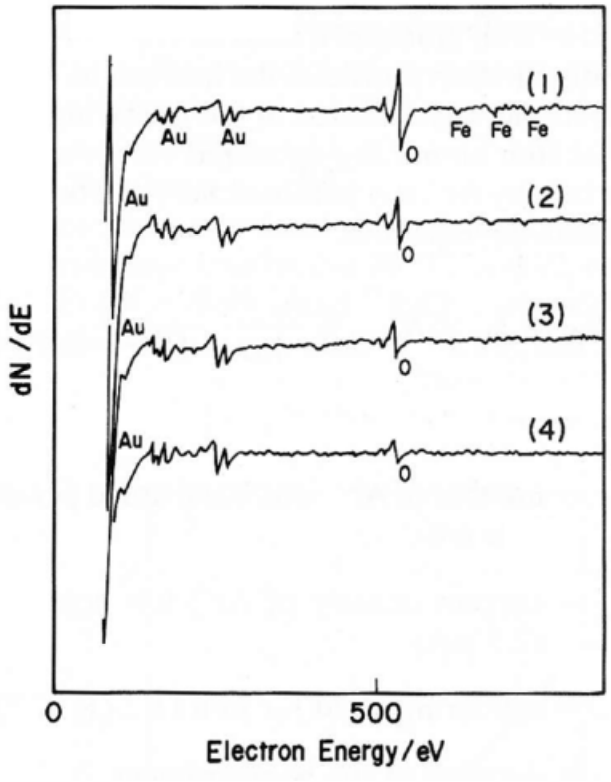

Fig. 4. The AES spectra in the electrode close to the surface after the electrolysis in the K2C03 solution: Ar^+ ion bombardment time, nothing (1), 30 s (2), 60 s (3), and 90 s (4).

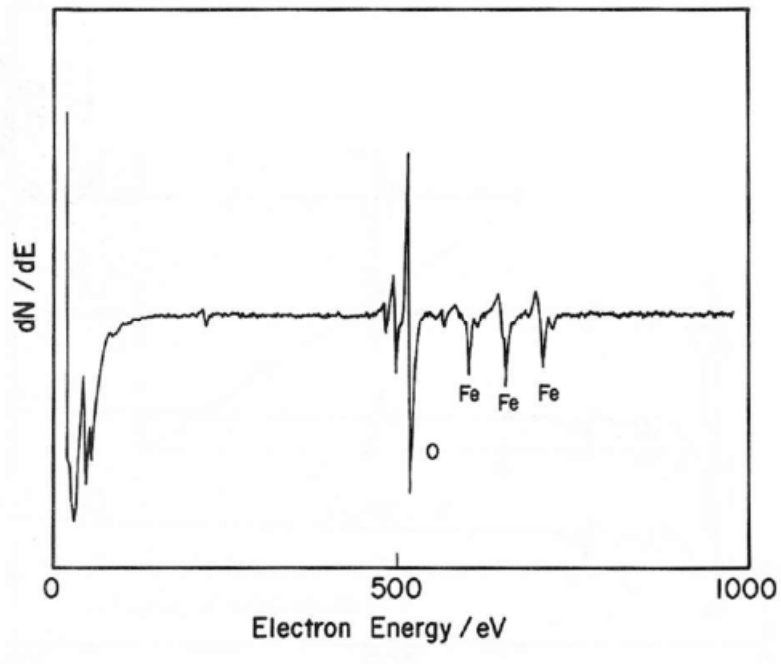

Fig. 5. The AES spectrum of a pure iron metal: Ar^+ ion bombardment time, 30 min.

The distribution profile of the iron atoms in the bulk of the electrode was obtained in the following way. The number of iron atoms N_{Fe} sputtered off from the electrode surface by Ar^+ ion bombardment can be estimated by the following equation:

$$N_{\mathrm{Fe}} = f_{\mathrm{Fe}} \times N_{Ar+} = \frac{f_{\mathrm{Fe}} \times I_{Ar+} \times t}{1.6 \times 10^{-19}}, \quad (2)$$

where

$N_{\mathrm{Ar}}+$ = number of Ar^+ ions bombarded per unit surface area

$I_{\mathrm{Ar}}+$ = current density of Ar^+ ion bombardment (2.5 μA)

f_{Fe} = sputtering yield for iron [1.2 (Ref. 7)]

t = duration of the bombardment.

The number of the atomic layers of iron layers sputtered off was estimated approximately from $N_{\mathrm{Fe}}/10^{15}$.

The typical distribution profile of iron atoms calculated from the results in Fig. 3 is shown in Fig. 6. The iron atoms occupied 44% of the top surface, which was distributed among ~100 layers (corresponding to ~5 min of bombardment time). Figure 7 shows the EPMA image of the iron atoms in the gold electrode after electrolysis in the Na_2SO_4 solution; we can see that the iron atoms were distributed uniformly over the entire electrode. The amounts of iron atoms produced in the gold electrodes in the various electrolyte solutions ranged between 1.0×10^{15} and 1.8×10^{16} atom/cm^2 (true area). The latter value shows that the total amount of iron produced on this electrode was ~17 μg. However, in the case of the gold electrodes without any mechanical treatment, the amount of iron atoms is two orders of magnitude smaller, ranging from 2.4×10^{14} to 8.0×10^{14} atom/cm^2 under the same electrolysis condition. This result suggests that the production of iron atoms is strongly affected on the crystal lattice strain of the electrode.

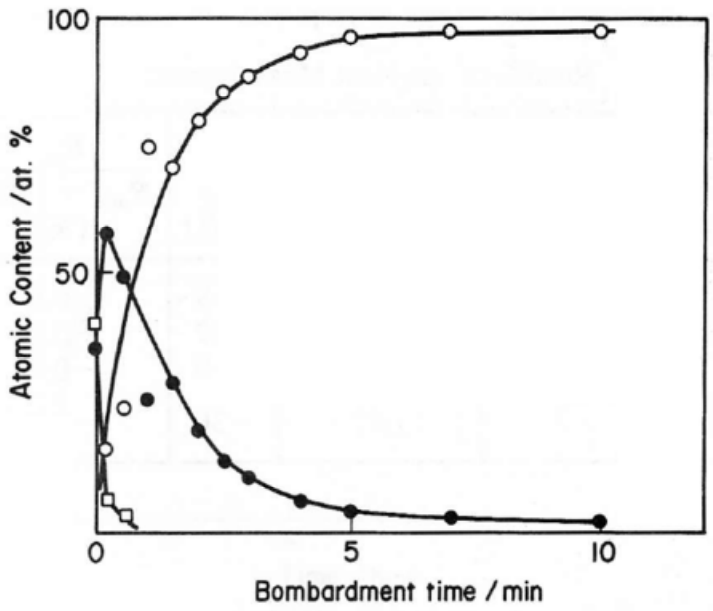

Fig. 6. The distribution profile of the iron atoms in the bulk of the electrode after the electrolysis in the Na_2SO_4 solution: iron is designated by the closed circles, platinum is designated by the open squares, and gold is designated by the open circles.

Figure 8 shows the relationship between the total amount of iron atoms and the mean R_{ex} obtained in every electrode/electrolyte system. Although the data were rather scattered, there seemed to be a linear relationship between these two parameters. This supports strongly the notion that iron atom production is related to excess energy evolution.

Isotopic Abundance of Iron Atoms

The SIMS measurement was made with an electrode after the electrolysis in the Na_2SO_4 solution. Figure 9 shows the SIMS spectra of the particles with mass numbers up to 200 caused by the first scanning. Figure 9 shows the spectra of Na^+, Al^+, Si^+, K^+, Ca^+, Ti^+, and Cr^+, which could not be detected by the AES measurement, were also observed to some extent other than those of Fe^+. This is probably due to the high sensitivity of SIMS for these elements. The spectrum of Cs^+ is attributed to a trace of cesium that remained in the vacuum chamber itself. The profile of the isotopic abundance of the iron atoms in the gold electrode is shown in Fig. 10. The iron atoms detected at the 15th scanning corresponds to those present in ~180 monolayers from the electrode surface.

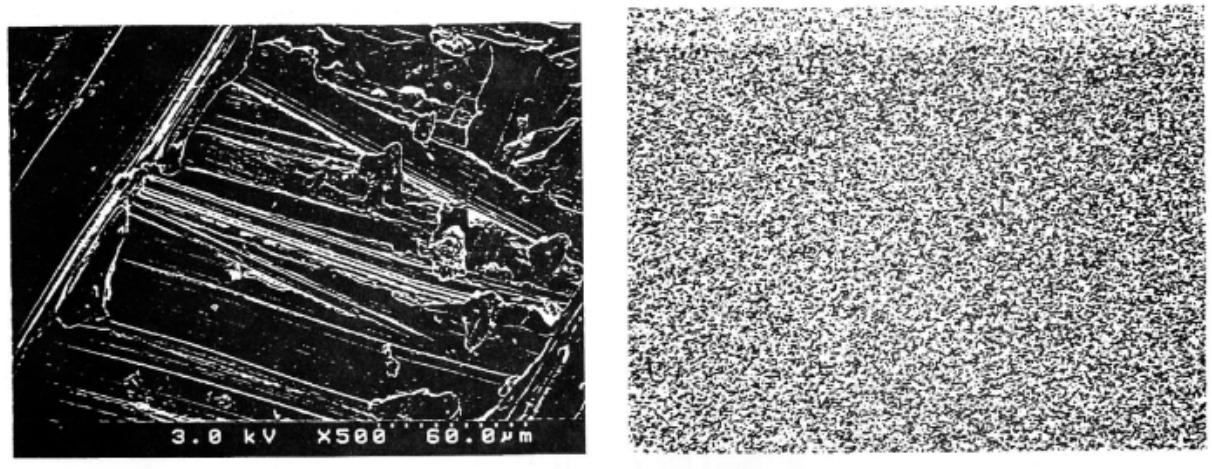

(a) (b)

Fig. 7. The SEM and EPMA images of the distribution of the iron atoms for the electrode after the electrolysis: (a) SEM image and (b) EPMA image (wavelength of X ray: 1.937 Å).

The rates of the content of the particles with mass numbers 54, 56, 57, and 58 corresponding to the iron isotopes obtained from the spectra of the first scan are 6.5, 77.5, 14.5, and 1.5%, respectively, which is clearly different from the natural isotopic abundance of the iron atoms. In particular, the difference is remarkable for particles with mass number 57, whose content is ~6.6 times the natural isotopic abundance of ^{57}Fe. The content of the particles with mass number 54 is also increased to some extent—perhaps because of the mixing of ^{54}Cr. On the other hand, the content of particles with mass number 56 is decreased by 15.5% from the natural isotopic abundance of 56Fe. Such a departure becomes significant with the increasing scan number. Eventually, the content of the particles of mass number 57 after 10 scans (corresponding to >120 layers from the electrode surface) reaches 25%, which is ~11 times the natural isotopic abundance of ^{57}Fe.

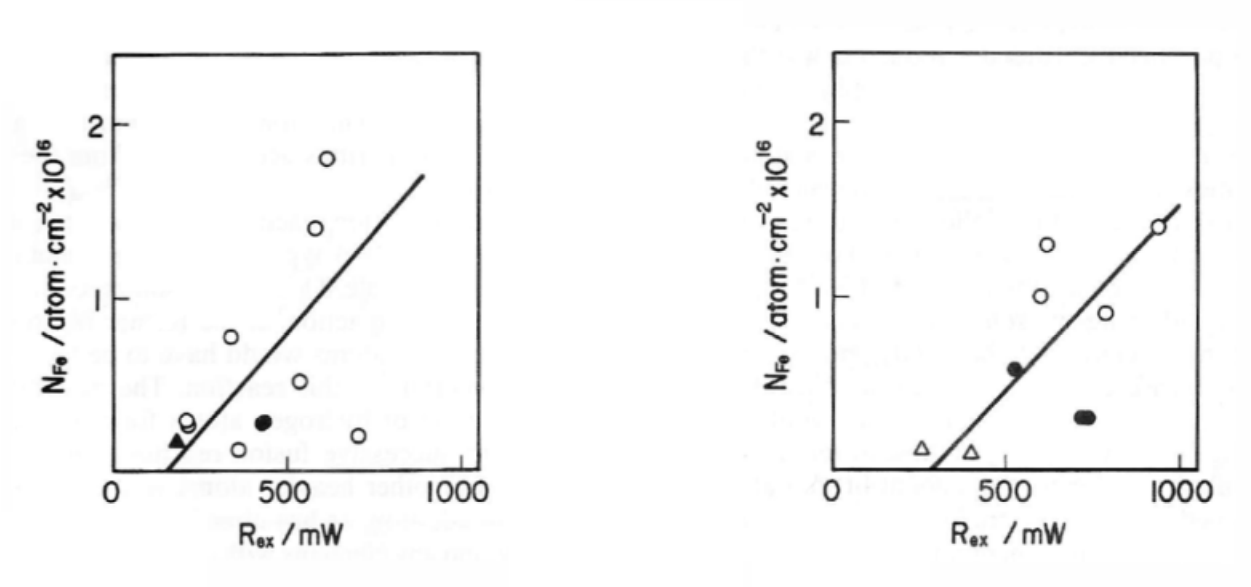

(a) (b)

Fig. 8. The total amounts of iron atoms plotted against the mean excess energy for an electrode (a) 5 cm2 and (b) 2.5 cm2; Na2SO4 is designated by the open circles, K2CO3 is designated by the closed circles, K2SO4 is designated by the open triangles, and KOH is designated by the closed triangles.

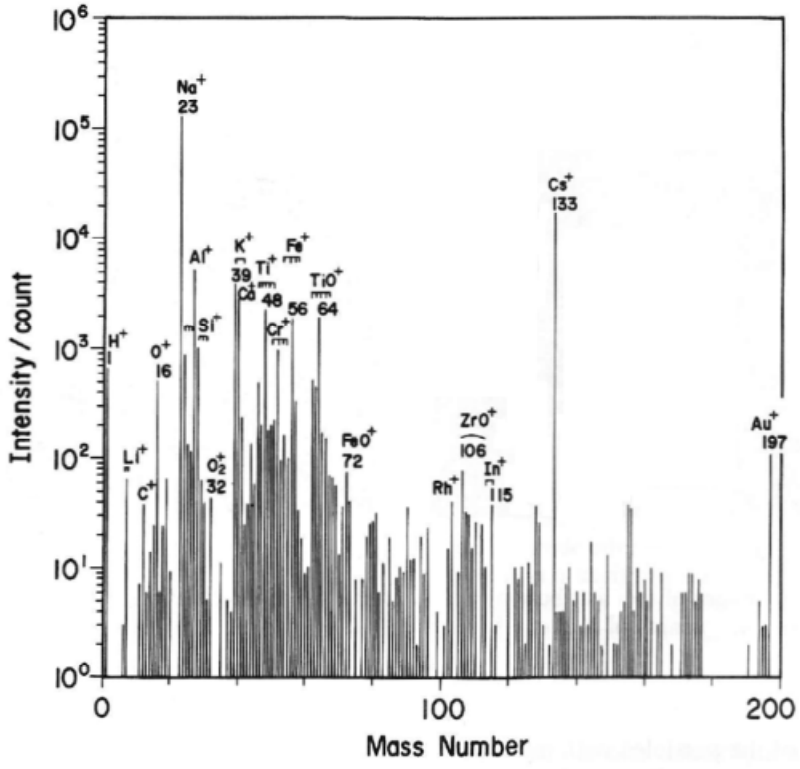

Fig. 9. The SIMS spectrum in the uppermost layers of the electrode after the electrolysis in the Na2SO4 solution.

Almost the same results are also obtained from the spectra with mass numbers of 70, 72, and 73, corresponding to $^{54}FeO^+$, $^{56}FeO^+$, and $^{57}FeO^+$, respectively, if all the particles with mass numbers 54, 56, and 57 are iron atoms. The ionic intensity ratios of mass number 57 to mass number 56 and of mass number 73 to mass number 72 are plotted against the scan numbers in Fig. 11. Although the plots are scattered, these two ratios can be seen on the whole to be in agreement. Therefore, the change in the content of the particles with mass numbers 54, 56, and 57 shown in Fig. 8 is not due to FeH^+ formation. From this fact, one may safely say that "heavy iron" was produced and that its production was the result of some nuclear transmutation occurring by the light water electrolysis.

The possibility of the formation of iron atoms from the impurities of chemical reagents or cell materials would be negligible because of the following reasons. First, the number of iron atoms from the reagent should be at most 7×10^{14} atoms, e.g., in 100 ml of 0.5 *M* Na_2SO_4 (Merck Spurapur-grade reagent) solution, because the concentration of iron is clarified to be <0.01 ppm according to the ICPMS measurement. Second, the number of iron atoms coming from the electrode materials would be negligible judging from the purity of these materials and their slight solubilities. Hence, the amount of iron atoms actually formed in a gold electrode by the electrolysis is at least one to two orders of magnitude larger than the values estimated earlier. Even if all the iron atoms coming from reagents and electrode materials are accumulated on/in the gold electrode, they would not have any influence on the AES signals of the iron shown in Fig. 3. From this point of view, most of the ^{56}Fe atoms, which are still the major isotopic component, are considered to be the product of nuclear transmutation.

The isotopic content of magnesium, silicon, potassium, calcium, titanium, chromium, and iron obtained from the spectra of the first, second, and third scans are listed in Table III together with the natural isotopic abundances and ionic intensities. As one can see, the isotopic contents of the elements other than iron are in agreement with these natural isotopic abundances within the limits of error. Therefore, these elements can be regarded as the impurities accumulated from the electrolyte solution.

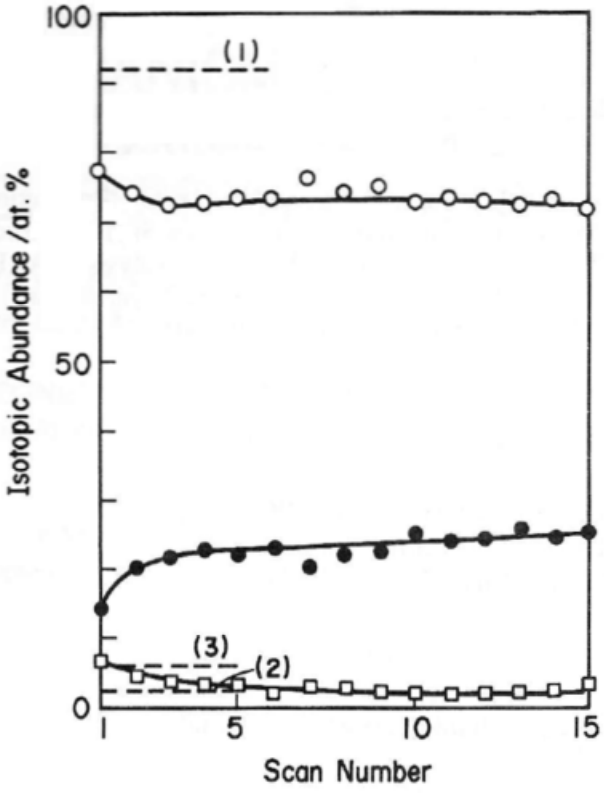

Fig. 10. The profile of the isotopic abundance of the iron atoms produced against the scan number of SIMS; for the solid lines, the rate of the content of the particles of mass numbers 56, 57, and 54 are designated by open circles, closed circles, and open squares, respectively, and for the dashed line, the natural isotopic abundance levels of ^{56}Fe, ^{57}Fe, and ^{54}Fe are designated by (1), (2), and (3), respectively.

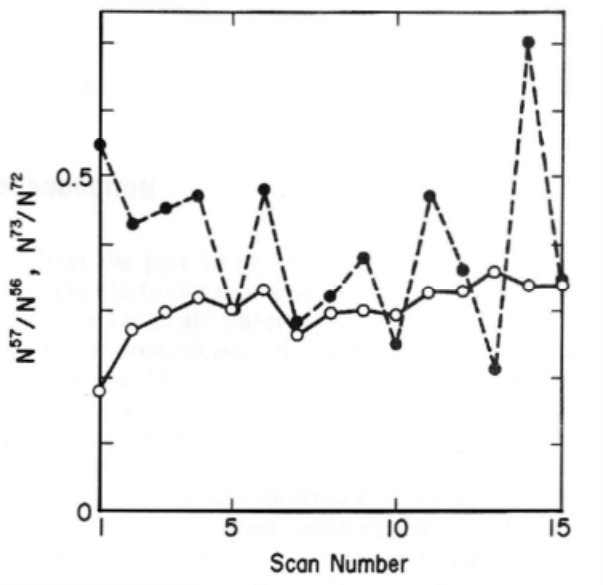

Fig. 11. The signal intensity ratios of mass number 57 to mass number 56 (open circles) and of mass number 73 to mass number 72 (closed circles).

TABLE III
Isotopic Content of Several Elements by SIMS Analysis

Element	Mass Number	Signal Intensity[a] (count)	Atomic Content (%) Scan Number			Natural Isotopic Abundance (%)
			1	2	3	
Magnesium	24	854	77.1	80.5	80.5	78.70
	25	135	12.2	8.9	9.2	10.13
	26	119	10.7	10.6	10.3	11.17
Silicon	28	1001	90.8	89.4	89.3	92.21
	29	62	5.6	5.9	5.5	4.68
	30	40	3.6	4.7	5.2	3.09
Potassium	39	3720	93.9	92.0	94.1	92.21
	41	240	6.1	8.0	5.9	6.88
Calcium	40	2746	94.7	95.5	95.9	96.97
	42	24	0.8	0.8	0.8	0.64
	44	131	4.5	3.7	3.3	2.06
Titanium	46	463	14.4	12.6	10.4	7.93
	47	203	6.3	7.2	7.0	7.28
	48	2173	67.6	69.2	73.1	73.94
	49	180	5.6	5.3	5.1	5.51
	50	197	6.1	5.6	4.4	5.34
Iron	54	163	7.0	4.5	3.6	5.82
	56	1816	77.4	74.3	73.2	91.66
	57	333	14.2	20.1	21.8	2.19
	58	33	1.4[b]	1.1[b]	1.4[b]	0.33

[a] Data of first scan.
[b] Contains 58Ni.

The transmutation reaction to produce iron atoms remains unknown. Two types of the transmutation reactions are conceivable. One is a fusion reaction, and the other is a fission reaction. If the former reaction is accepted, hydrogen atoms would have to be thought of as starting materials of this reaction. The possibility of a fusion reaction of hydrogen atoms forming helium atoms and of successive fusion reactions producing carbon atoms or other heavier atoms would be extremely remote. In addition, as has already been mentioned, we could not find any elements with an unusual isotopic abundance in elements smaller than the iron present on/in the gold electrode after the electrolysis. More recently, we found considerable amounts of platinum and osmium with unusual isotopic abundances produced on/in the gold cathode electrolyzed with higher current densities.[8] This fact suggests that iron atoms are produced by some nuclear fission via platinum and osmium production starting from gold. To discuss this problem in detail, one must identify the intermediate elements participating in the iron production and assay these amounts.

REFERENCES

1. R. T. BUSH and R. D. EAGLETON, "Experiments Supporting the Transmission Resonance Model for Cold Fusion in Light Water: I. Correlation of Isotopic and Elemental Evidence with Excess Heat," *Proc. 3rd Int. Conf. Cold Fusion*, Nagoya, Japan, 1992, p. 405, Universal Academy Press.
2. R. T. BUSH, "A Light Water Excess Heat Reaction Suggests that 'Cold Fusion' May Be 'Alkali-Hydrogen' Fusion," *Fusion Technol.*, **22**, 301 (1992).
3. T. OHMORI and M. ENYO, "Excess Heat Produced During Electrolysis of H_2O on Ni, Au, Ag and Sn Electrodes in Alkaline Media," *Proc. 3rd Int. Conf. Cold Fusion*, Nagoya, Japan, 1992, p. 427, Universal Academy Press.
4. T. OHMORI and M. ENYO, "Excess Heat Evolution During Electrolysis of H_2O with Nickel, Gold, Silver, and Tin Cathodes," *Fusion Technol.*, **24**, 293 (1993).
5. T. OHMORI, "Measurement of the Potential of Zero Charge on Nickel Electrode by the Galvanostatic Transient Method," *J. Electroanal. Chem.*, **157**, 159 (1983).
6. A. TAKEUCHI, K. TANAKA, I. TOYOSHIMA, and K. MIYAHARA, "Catalysis and Coordinative Unsaturation of Active Sites on Sulfurated Nickel Catalyst," *J. Catalysis*, **40**, 94 (1975).
7. M. KAMINSKY, *Atomic and Ionic Impact Phenomena on Metal Surfaces*, Springer-Verlag, Berlin (1965).
8. T. OHMORI, T. MIZUNO, and M. ENYO, "Production of Heavy Metal Elements and the Anomalous Surface Structure of the Electrode During the Light Water Electrolysis on Au Electrode," *Proc. 6th Int. Conf. Cold Fusion*, Toya, Japan, 1996, Universal Academy Press (to be published).

Tadayoshi Ohmori (BS, chemistry, Hokkaido University, Japan, 1962; Dr., electrochemistry, Hokkaido University, Japan, 1988) is currently a research associate at the Catalysis Research Center of Hokkaido University. His current research interests are interfacial energy conversion and fuel cells.

Michio Enyo (BS, chemistry, Hokkaido University, Japan, 1953; PhD, electrochemistry, University of Pennsylvania, 1961) is currently president of the Hakodate National College of Technology. His current research interests are interfacial energy conversion and hydrogen electrosorption in metal.

Tadahiko Mizuno (BS, 1968; Msci, 1970; and Dr, 1973, applied physics, Hokkaido University, Japan) is currently a research associate of the faculty of engineering at Hokkaido University. His current research interests are hydrogen storage materials and localized corrosion.

Yoshinobu Nodasaka (BS, biology, Hokkaido University, Japan, 1969) is currently a member of the technical staff at the School of Dentistry of Hokkaido University. His current research interest is the ultrastructure of materials.

Hideki Minagawa (BS, 1983; Msci, 1985; and Dr, 1988, nuclear technology, Hokkaido University, Japan) is currently a senior researcher at the Hokkaido National Industrial Research Institute. His current research interest is crystal production under microgravity conditions.